Radiology

Diffusion-weighted MRI for Unenhanced Breast Cancer Screening

Nita Amornsiripanitch, MD • Sebastian Bickelhaupt, MD • Hee Jung Shin, MD • Madeline Dang, MS • Habib Rahbar, MD • Katja Pinker, MD, PhD • Savannah C. Partridge, PhD

From the Department of Breast Imaging, University of Massachusetts Memorial Medical Center, Worcester, Mass (N.A.); Medical Imaging and Radiology–Cancer Prevention, German Cancer Research Center, Heidelberg, Germany (S.B.); Department of Radiology, Asan Medical Center, University of Ulsan, Seoul, South Korea (H.J.S.); Department of Radiology, University of Washington, 825 Eastlake Ave E, G2-600, Seattle, WA 98109 (M.D., H.R., S.C.P.); Department of Radiology, Memorial Sloan-Kettering Cancer Center, New York, NY (K.P.); and Department of Biomedical Imaging and Image-guided Therapy, Medical University of Vienna, Vienna, Austria (K.P.). Received December 6, 2018; revision requested February 11, 2019; final revision received June 18; accepted July 10. **Address correspondence to** S.C.P. (e-mail: *scp3@uw.edu*).

S.C.P. supported in part by the National Cancer Institute (R01CA207290).

Conflicts of interest are listed at the end of this article.

Radiology 2019; 293:504–520 • https://doi.org/10.1148/radiol.2019182789 • Content codes: BR MR OI

Diffusion-weighted (DW) MRI is a rapid technique that measures the mobility of water molecules within tissue, reflecting the cellular microenvironment. At DW MRI, breast cancers typically exhibit reduced diffusivity and appear hyperintense to surrounding tissues. On the basis of this characteristic, DW MRI may offer an unenhanced method to detect breast cancer without the costs and safety concerns associated with dynamic contrast material–enhanced MRI, the current reference standard in the setting of high-risk screening. This application of DW MRI has not been widely explored but is particularly timely given the growing health concerns related to the long-term use of gadolinium-based contrast material. Moreover, increasing breast density notification legislation across the United States is raising awareness of the limitations of mammography in women with dense breasts, emphasizing the need for additional cost-effective supplemental screening examinations. Preliminary studies suggest unenhanced MRI with DW MRI may provide higher sensitivity than screening mammography for the detection of breast malignancies. Larger prospective multicenter trials are needed to validate single-center findings and assess the performance of DW MRI for generalized breast cancer screening. Standardization of DW MRI acquisition and interpretation is essential to ensure reliable sensitivity and specificity, and an optimal approach for screening using readily available techniques is proposed here.

Online supplemental material is available for this article.

In combination with improved treatments, screening mammography is responsible for a substantial decline in breast cancer mortality over the past 4 decades (1). However, it has been recognized that mammography is less effective in some populations (2). For example, mammography's reduced sensitivity of breast cancer detection in patients with dense breasts, even when performed with digital breast tomosynthesis, has led to federal and state breast density notification legislation. Furthermore, some women, regardless of breast density, are at higher lifetime risk to develop breast cancer and may benefit from supplemental screening examinations (3). As health care moves toward personalized patient-centered care, many imaging techniques have been proposed as potential supplemental screening tools to mammography.

One of the mostly widely explored modalities for supplemental screening is dynamic contrast material–enhanced (DCE) MRI. Owing to its high sensitivity and proven ability to depict additional cancers (4), DCE MRI is recommended by national and international screening policy guiding organizations as a supplemental screening tool for women at high risk for breast cancer (3,5). However, DCE MRI is limited by high costs, preventing widespread use in women with low to moderate risk for breast cancer. High cost is attributable both to lengthy examination times and cost of contrast material administration, which includes costs for the gadolinium agent, intravenous supplies, point-of-care renal function screening, intravenous placement and monitoring, and on-site physician coverage for adverse contrast material–related events. As a result, the 2019 national Medicare reimbursement for DCE MRI is 58% higher than that of a noncontrast breast MRI ($410.49 vs $259.84) (6).

Abbreviated breast MRI has been proposed to partially solve the cost problem DCE MRI poses by reducing imaging time. Typical abbreviated MRI protocols include only pre- and immediate postcontrast sequences, omitting the additional delayed contrast-enhanced sequences mandated by American College of Radiology accreditation guidelines (7) and other optional sequences such as a precontrast non–fat-suppressed T1 series to reduce imaging times to less than 10 minutes. Multiple studies have shown equivalent cancer detection rates, positive predictive values, and/or negative predictive values versus complete conventional protocols (8–10). However, abbreviated breast MRI still requires administration of intravenous gadolinium-based contrast material. Aside from the disadvantages of cost and pain of venipuncture, intravenous contrast material use is contraindicated in pregnancy and patients with renal impairment or gadolinium contrast material allergy (11–13). Furthermore, there are growing public concerns over the unknown health effects of gadolinium deposition in brain and other tissues from repeated gadolinium contrast agent injection, which must be considered in an asymptomatic

Abbreviations

ADC = apparent diffusion coefficient, DCE = dynamic contrast enhanced, DCIS = ductal carcinoma in situ, DW = diffusion weighted, EPI = echo-planar imaging

Summary

Diffusion-weighted MRI is a fast, unenhanced modality that shows promise in identifying mammographically occult malignancy and warrants further investigation as an alternative supplemental breast cancer screening tool.

Essentials

- Diffusion-weighted (DW) MRI is a fast, unenhanced technique that demonstrates breast malignancies based on reduced water diffusivity relative to normal tissue.
- DW MRI can help distinguish between benign and malignant lesions in the diagnostic setting, and there are emerging data that DW MRI could also serve as part of a non–contrast-enhanced MRI approach for screening with sensitivity lower than that of dynamic contrast-enhanced MRI but superior to that of mammography.
- Breast DW MRI approaches vary widely and there is need for technique standardization. Suggested DW MRI acquisition and interpretation protocols are suggested for a screening application based on current literature.
- Advanced DW MRI acquisition and postprocessing techniques may improve imaging quality and sensitivity in cancer detection.

and relatively young population such as those receiving breast cancer screening (14–16).

In light of 38 states with breast density notification laws and federal breast density notification laws, whole-breast US has become widely adopted as a supplemental screening tool for women with dense breasts owing to its relative ubiquity and low cost despite no definitive recommendation by any major medical organization (17,18). Whole-breast US also requires no contrast agent administration or radiation. However, questions remain as to whether the low positive predictive value of US and corresponding high negative biopsy rate will render the method cost-ineffective and increase patient anxiety toward US screening in the long run (19–21).

Given the limitations of available supplemental screening modalities, there is benefit in identifying a safe and cost-effective alternative implementable on a broad scale. While the authors recognize other modalities are being explored as possible supplementary screening tools (including contrast-enhanced digital mammography, PET, and ^{99m}Tc-sestamibi–based molecular breast imaging, each of which utilize ionizing radiation), this review focuses on diffusion-weighted (DW) MRI's potential as a stand-alone breast cancer screening modality, reviewing results of blinded studies (22–27) and presenting practical applications using readily available techniques.

DW MRI in Breast Cancer

DW MRI is a fast, widely available, unenhanced MRI technique. Unlike DCE MRI, which relies on administration of an intravascular gadolinium-based contrast agent to illustrate tissue perfusion, DW MRI measures endogenous water movement within tissue. Motion-sensitizing gradients are applied during image acquisition, and the DW signal intensity is proportional to water mobility within a voxel, as described by the general equation:

$$S_D = S_0 e^{-b*ADC},$$

where S_D is the diffusion-weighted signal intensity, S_0 is the signal intensity without diffusion weighting, b or "b value" is the diffusion sensitization factor, which varies by the strength and timing of the applied diffusion gradients (in sec/mm^2), and the apparent diffusion coefficient (ADC) is the rate of diffusion defined as the average area occupied by a water molecule per unit time (in mm^2/sec). An ADC map can be calculated using image acquisitions at two or more different b values, quantitatively reflecting a composite of tissue factors affecting net water mobility in each voxel including microcirculation, cellular density, organization, and membrane integrity (28).

Differential Diagnosis of Suspicious Breast Lesions

Numerous studies have demonstrated breast malignancies to exhibit impeded water diffusion, reflected by lower ADC and higher DW MRI signal compared with normal surrounding breast tissue (29) (Fig 1). Although cellularity may play a role in diffusion impedance, the correlation has found to be inconsistent and/or modest (30–32), suggesting a more complex relationship between ADC and tissue microenvironment. Initial exploration of DW MRI performance focused on the diagnostic value of DW MRI as a supplement to DCE MRI to improve DCE MRI's relatively modest specificity compared with mammography (33,34). In a meta-analysis compiling 14 studies between 2008 and 2014 investigating DW MRI as a supplement to DCE MRI, quantitative ADC measures from DW MRI alone could differentiate benign versus malignant lesions with pooled sensitivity and specificity of 86.0% and 75.6%, respectively, compared with 93.2% and 71.1% for DCE MRI alone (35). Although the study concluded that combined use of DW MRI and DCE MRI yielded the best performance (sensitivity and specificity of 92% and 86%, respectively), it is worth noting that DW MRI alone had comparable diagnostic performance to that of DCE MRI for differentiating known suspicious lesions.

Potential for Detecting Breast Malignancies without Contrast Enhancement

Considering the limitations of DCE MRI in length, cost, and contrast material–related safety, DW MRI could be a useful stand-alone screening tool if proven to supplement mammography and outperform other supplemental screening modalities for cancer detection. In a study of 118 mammographically occult lesions, 89% of DCE MRI–detected malignancies were visible at DW MRI (36). Additionally, DW MRI may be superior to US at detecting mammographically occult cancer. In another study of 60 mammographically occult cancers, DW MRI potentially detected more cancers than MRI-guided focused US (78% vs 63%, respectively, P = .049, Fig 2) (37). Another benefit of DW MRI is that lesion detection remains independent of background parenchymal enhancement, breast density, menopausal status, or

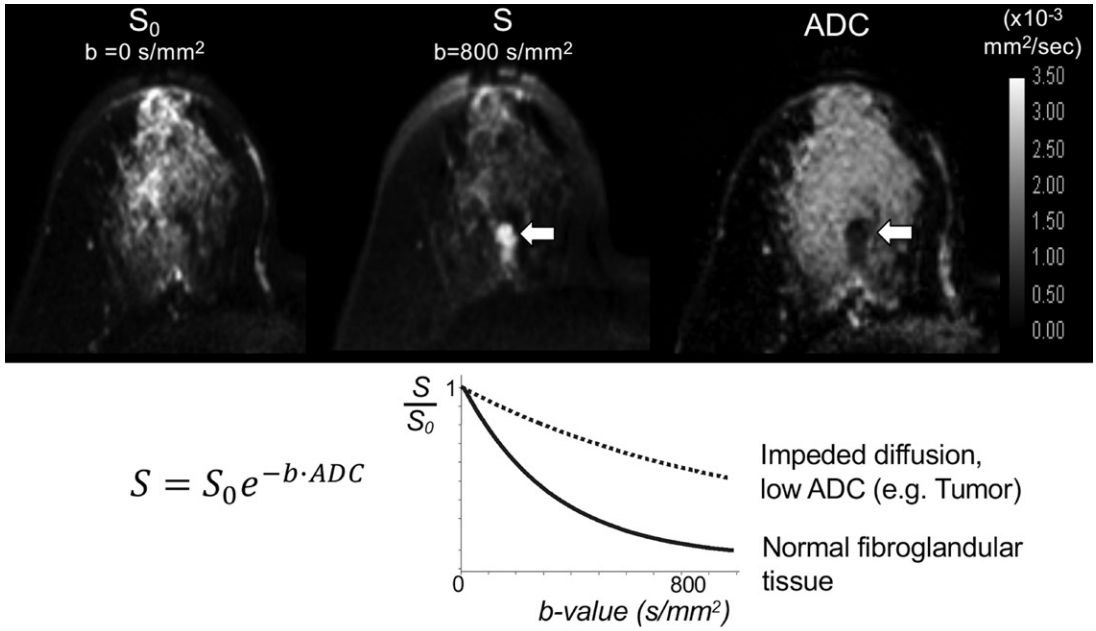

Figure 1: Images in 52-year-old woman with mammographically dense breasts and invasive ductal carcinoma in the right breast. On (top) images from axial noncontrast diffusion-weighted (DW) MRI examination, the lesion is not visible on (left) the T2-weighted (b = 0 sec/mm^2) image, but it is readily apparent as hyperintense to surrounding fibroglandular breast tissue on (center) b = 800 sec/mm^2 DW MR images (arrow) because of impeded diffusion in the lesion. The corresponding apparent diffusion coefficient (ADC) map (right) confirms lower diffusivity in the lesion (arrow) (mean ADC = 0.89 × 10^{-3} mm^2/sec) compared with normal tissue (mean ADC = 2.21 × 10^{-3} mm^2/sec). The b value (in seconds per square millimeter) describes the degree of diffusion sensitization applied during DW MRI. As illustrated on (bottom) the plot of signal intensity versus b value for the monoexponential decay model (where the DW signal intensity S is expressed in terms of S_0, the signal intensity without diffusion weighting, b value, and ADC), at higher b values the differences in signal decay between cancer with reduced ADC (dotted curve) and normal fibroglandular tissues (solid curve) can be exploited to increase contrast on DW MRI of cancerous lesions relative to other breast tissues and to improve detectability.

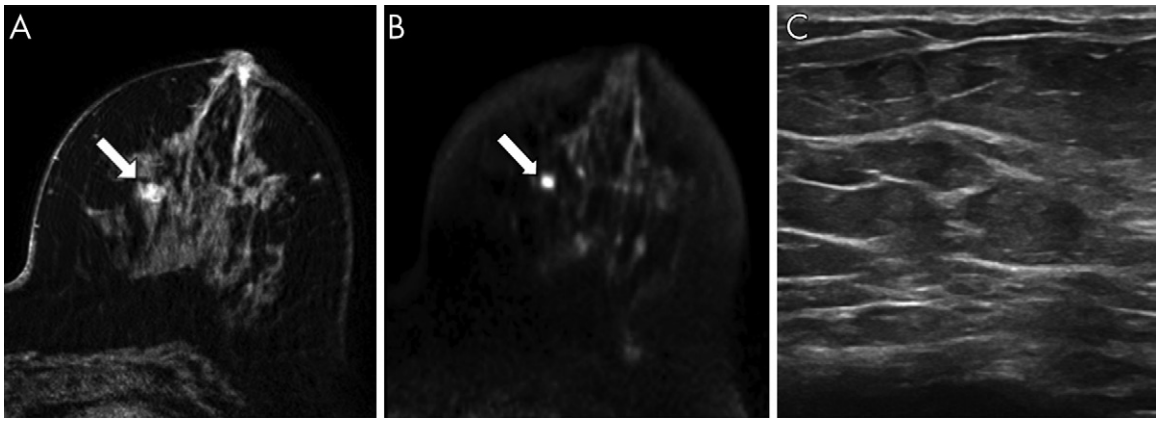

Figure 2: *A–C,* Images in 75-year-old woman with invasive ductal carcinoma (grade 1) detected at bilateral 3.0-T breast MRI for high-risk screening. *A,* Axial image from dynamic contrast-enhanced MRI shows an oval mass (arrow) with irregular margins in the left breast at 9 o'clock, middle depth, 47 mm from the nipple measuring 7 × 6 × 11 mm. *B,* At axially acquired diffusion-weighted MRI (b = 800 sec/mm^2), the lesion (arrow) was hyperintense and was deemed visible by three readers. The apparent diffusion coefficient was 0.83 × 10^{-3} mm^2/sec. *C,* Image from subsequent targeted US showed no correlate. (Reprinted, with permission, from reference 37.)

timing during menstrual cycle, all factors which influence mammographic and/or DCE MRI lesion detection (38,39).

It is important to note that readers were not blinded to images from DCE MRI when identifying mammographically occult cancers with DW MRI and US in these preliminary studies. Therefore, they do not reflect the real-world performance of DW MRI in the clinical setting.

Blinded DW MRI Reader Studies

To date, several studies have explored reader performance for cancer detection using unenhanced MRI with DW MRI, which overall demonstrated readers' ability to visually identify malignancy at DW MRI with promising sensitivity and specificity (22–27,40–48). Of those, six studies included patients with both positive and negative imaging findings and/or healthy controls

Table 1: Summary of Blinded Reader Studies Evaluating DW MRI Performance for Breast Cancer Screening

Study	Total No. of Women	Cancer Prevalence (%)*	Mean Cancer Size (mm)	Field Strength (T)	DW MRI Voxel Size (mm)	Max *b* Value (sec/mm²)	NC MRI Sequences Evaluated	Study Population	Sensitivity (%)†	Specificity (%)	PPV (%)	NPV (%)
Yabuuchi 2011 (27)	63	67 (42/63)‡	20 (invasive) 23.5 (in situ)	1.5	2.8 × 4 × 5	1000	ssEPI, T2 weighted	Asymptomatic women with dynamic contrast-enhanced MRI–detected malignancy and negative and benign control subjects	50	95	95	49
Kazama 2012 (23)	46	27 (25/92)§	NA (range, 1–20)	1.5	1.8 × 3 × 5	800	ssEPI, T2 weighted, ADC‖	Patients > 50 years with known malignancy and healthy control subjects	74	93	93	75
Trimboli 2014 (26)	67	32 (37/116)§	20	1.5	2.7 × 2.7 × 4	1000	ssEPI, T1 weighted, STIR, ADC	Patients with known malignancy, suspicious mammographic or US findings, and intermediate-to-high–risk screening	77 (76–78)#	90 (90–90)#	74	89
Telegrafo 2015 (25)	280	46 (129/280)‡	18	1.5	3.1 × 3.1 × 3	1000	DWIBS, T2 weighted, STIR, ADC‖	Patients with suspicious mam mographic or US findings and high-risk screening	94	79	79	94
McDonald 2016 (24)	48	25 (24/95)§	10**	1.5, 3	1.9 × 1.9 × 5 (at 1.5 T) or 1.5 × 1.5 × 5 (at 3.0 T)	600, 800	ssEPI, T2 weighted, T1 weighted, ADC	High-risk women with dense breast tissue: 50% with occult cancer at mammography and 50% matched negative control subjects	45	91	63	81
Kang 2017 (22)	343	2.5 (9/358)††	18 (invasive) 19 (in situ)	3‡‡	1.7 × 1.7 × 3	1000	rs-EPI MIP, rs-EPI fused to T1 weighted	Asymptomatic women with history of breast cancer and no known active malignancy	93# (89–100)#	94# (93–95)#	30	99.7

Note.—ADC = apparent diffusion coefficient, DWIBS = diffusion-weighted MRI with background suppression, MIP = maximum intensity projection, NA = not available, NC = nonenhanced, rs-EPI = readout-segmented echo-planar diffusion-weighted imaging, ssEPI = single-shot echo-planar imaging, STIR = short inversion time inversion recovery.

* Data in parentheses are raw data. Cancer prevalence calculations varied by study (and were based on patients, examinations, breasts, or lesions, as noted) to match the performance metrics reported in the study.

† Data in parentheses are ranges.

‡ Prevalence and performance metrics were calculated per patient.

§ Prevalence and performance metrics were calculated per breast (only one breast was evaluated for some patients because of prior mastectomy or lack of follow-up information).

‖ Quantitative ADC measurement was used as part of unenhanced imaging analysis.

Mean sensitivities and specificities for multiple readers were not reported in the original literature and were calculated for this review.

** Median reported.

†† Prevalence and performance metrics were calculated per examination (some patients underwent multiple examinations)

‡‡ Per direct communication by authors.

Table 2: False-Negative and False-Positive Rates of Blinded Reader Studies Evaluating DW MRI Performance for Breast Cancer Screening

Study	Total No. of Women	Total No. of Cancers	False-Negative Findings		False-Positive Findings	
			No. of Findings	Description of Findings (If Reported)	No. of Findings	Description of Findings (If Reported)
Yabuuchi 2011 (27)	63	42	21	NA	1	NA
Kazama 2012 (23)	46	25	6.5*	Cancer < 10 mm; cancer with calcifications	5*	Vessel; artifact; glandular tissue
Trimboli 2014 (26)	67	37	8.5*	NME (n = 3); mass (n = 5.5)*	8*	Normal tissue; lobular intraepithelial neoplasia; granulomatous mastitis
Telegrafo 2015 (25)	280	129	8	Mucinous carcinoma (n = 4); DCIS (n = 4)	32	Cysts (n = 12); fibrotic areas (n = 6); fibroadenolipoma (n = 4); fibroadenoma (n = 6); typical hyperplasia (n = 4)
McDonald 2016 (24)	48	24	10.7* (Note: all cancers in this study were mammographically occult)	IDC (n = 4); ILC (n = 1); DCIS (n = 3)	6*	Fibroadenoma; proteinaceous cyst; artifact; asymmetric signal intensity because of prior treatment of contralateral breast or other factors
Kang 2017 (22)	343	10	1.3*	NA	5.4%*†	NA

Note.—NA = not available, NME = nonmass enhancement, DCIS = ductal carcinoma in situ, IDC = invasive ductal carcinoma, ILC = invasive lobular carcinoma.

* Average between multiple readers.

† Only percentage (no raw number) was reported.

in their cohorts, therefore most closely simulating a screening population (22–27). Although study designs varied, in general, readers retrospectively assessed only unenhanced MRI sequences and did not review the contrast-enhanced sequences. These included a DW MRI sequence with or without nonenhanced T1- or T2-weighted sequence. Readers assigned a numerical scale according to level of suspicion for malignancy, comparable to the Breast Imaging Reporting and Data System categories, or a qualitative positive or negative assessment. In some studies, results were then compared with assessments on mammogram and/or contrast-enhanced MRI performed by either the same readers (after a washout period) or another set of readers.

Most notably, Kang et al included 343 consecutive asymptomatic patients with previous history of breast cancer presenting for DCE MRI screening (22), representative of an intermediate-risk screening population of women with elevated risk for cancer recurrence but who may not meet criteria for high-risk (>20% lifetime risk) DCE MRI supplemental screening (49). With 2.5% cancer prevalence, this reader study most closely evaluated DW MRI performance in a true screening population. The remaining five studies also included asymptomatic MRI screening patients and/or healthy controls but enriched their patient cohorts with a higher rate of cancers (with cancer prevalence ranging 25%–67%). However, to simulate a screening experience, readers in most studies were blinded to clinical history and other imaging modalities, and, therefore, blinded to cancer prevalence in the study populations. McDonald et al and Yabuuchi et al retrospectively evaluated consecutive asymptomatic cancers detected at DCE MRI combined with negative controls from high-risk screening populations—controls were age matched in McDonald et al (24) whereas selected normal and benign high-risk screening patients were added to the cohort by Yabuuchi et al (27). The other studies did not restrict inclusion criteria to asymptomatic patients, also including patients undergoing MRI for known (23,26) or suspected (25,26) breast cancer.

In this group of studies, DW MRI sensitivities ranged between 45% and 94%, and specificity between 79% and 95% with means of 72% and 90%, respectively (Table 1). Notably, sensitivity was lowest in McDonald et al (45%), likely due to inclusion of only mammographically occult malignancies (with smaller median lesion size) and 1.5-T examinations without exclusion of examinations with poor image quality, unlike Kazama et al and Kang et al (22,23). The sensitivities in Kang et al (93%) and Telegrafo et al (94%) were higher than in other studies, which may be partially explained by their use of advanced readout-segmented echo-planar imaging (EPI) and DW MRI with background suppression techniques, respectively, versus conventional single-shot EPI DW MRI in the other studies. These advanced DW MRI methods could help to improve sensitivity through better image quality and lesion contrast, as described in more detail below (Advanced Techniques section).

False-Negative and False-Positive Findings at DW MRI

The number of false-negative and false-positive findings in the above-described studies, along with any available additional characteristics, are given in Table 2. Of note, the majority of false-positive and false-negative results were reported in the studies on a lesion rather than an examination level. Therefore, the number of true-positive and true-negative examinations are not available for accurate calculation of false-positive and false-negative rates, such as in mammographic auditing.

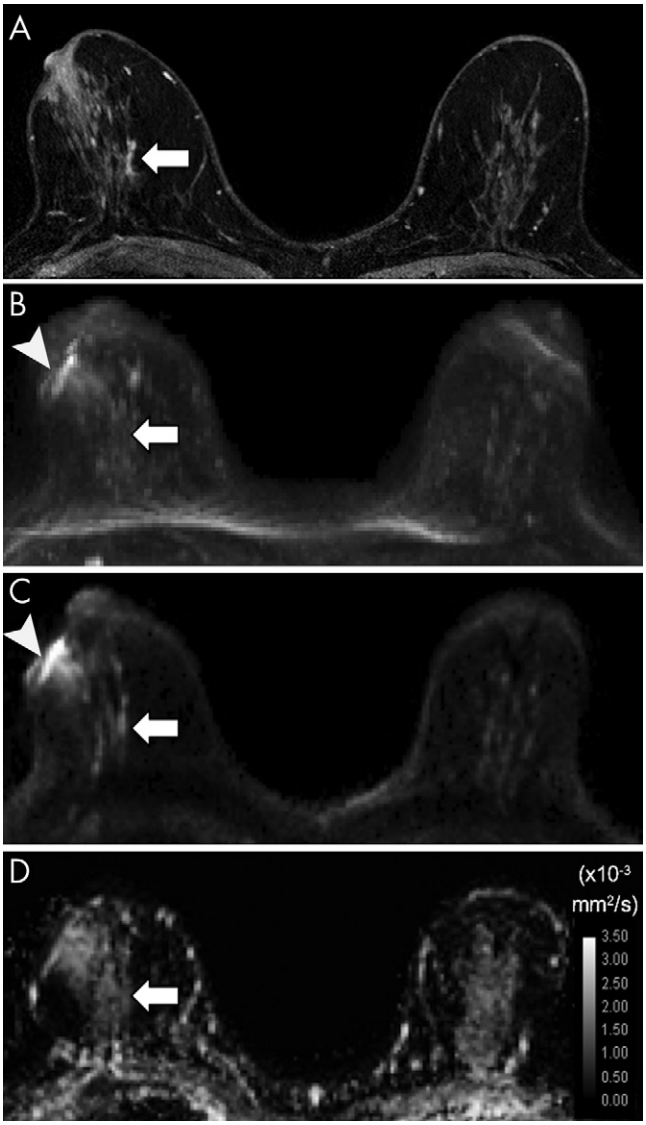

Figure 3: *A–D*, Axial images in 60-year-old woman with heterogeneously dense breasts and ductal carcinoma in situ in the right breast that was not detectable at diffusion-weighted (DW) MRI (and that represented a DW MRI false-negative finding). *A*, Image from 3.0-T dynamic contrast-enhanced MRI shows the lesion (arrow) as a 36-mm area of nonmass enhancement. On, *B*, a DW MRI maximum intensity projection obtained with a *b* value of 800 sec/mm^2 and, *C*, a representative single section from DW MRI obtained with a *b* value of 800 sec/mm^2, the lesion (arrow) is relatively isointense to nearby fibroglandular tissue and is not readily detectable, particularly because of the presence of a bright susceptibility artifact at the nipple (arrowhead). On, *D*, the apparent diffusion coefficient (ADC) map, the lesion (arrow) shows low mean ADC (1.27 × 10^{-3} mm^2/sec), but the ADC map does not aid in visual detection of the lesion.

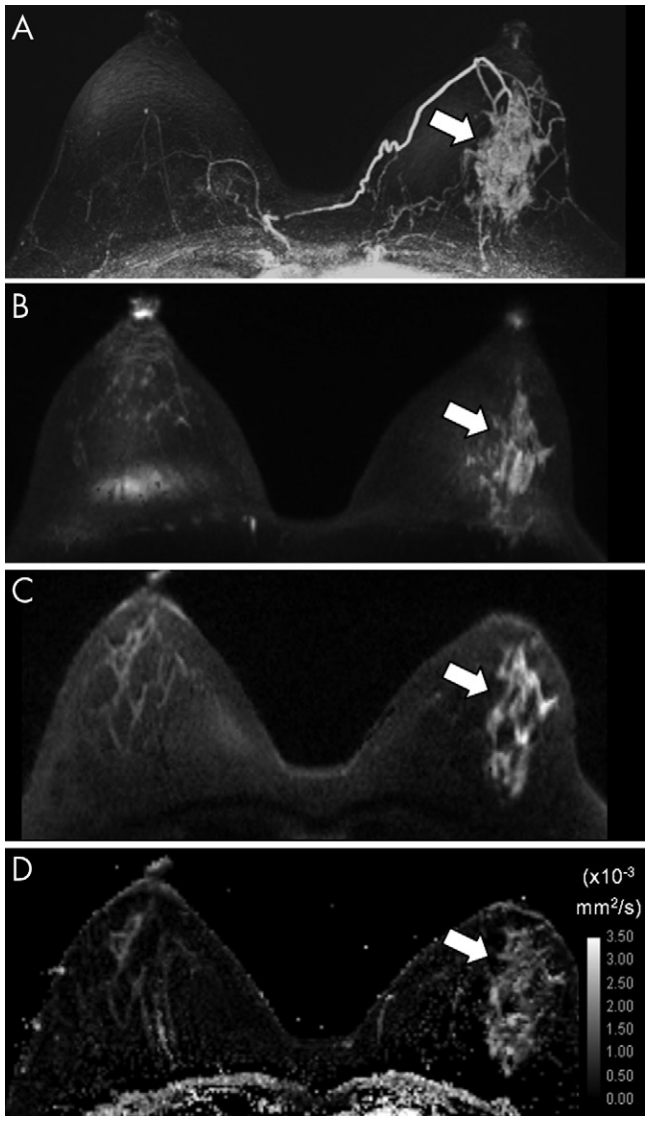

Figure 4: *A–D*, Axial images in 49-year-old woman with ductal carcinoma in situ in the left breast identified at 3.0-T dynamic contrast-enhanced and diffusion-weighted (DW) MRI (true-positive DW MRI examination). Shown are, *A*, a dynamic contrast-enhanced MRI postcontrast subtraction maximum intensity projection (MIP) depicting a 5.2-cm area of nonmass enhancement (arrow), *B*, a DW MRI MIP obtained with a *b* value of 1000 sec/mm^2, *C*, a representative single section through the lesion (arrow) obtained at DW MRI with a *b* value of 1000 sec/mm^2, and, *D*, the corresponding apparent diffusion coefficient (ADC) map, where the area of nonmass enhancement (arrow) exhibited a low mean ADC of 1.18 × 10^{-3} mm^2/sec.

False-Negative Findings

Literature suggests that ductal carcinoma in situ (DCIS) may be more difficult to detect at DW MRI than invasive disease. Among blinded reader studies evaluating DW MRI detection of malignancies that included DCIS (24–26,40–45,48), DCIS was more likely missed by DW MRI than invasive ductal carcinoma (average, 42; range, 14–100% versus 10, range, 0%–40%). Furthermore, readers in McDonald et al rated the conspicuity of invasive cancer as significantly higher than that of DCIS (4.0/5 versus 2.8/5) (24). In general, DCIS exhibits less diffusion impedance as reflected by higher ADC measurements, compared with invasive carcinomas (50), which may explain their relatively low conspicuity at DW MRI. Examples of DCIS that is not detectable (false-negative findings) versus readily visible at DW MRI are shown in Figure 3 and Figure 4, respectively. However, there are mixed reports regarding correlation between ADC and DCIS grade (50–52). Moreover, high-grade DCIS may actually exhibit lower qualitative DWI intensity and quan-

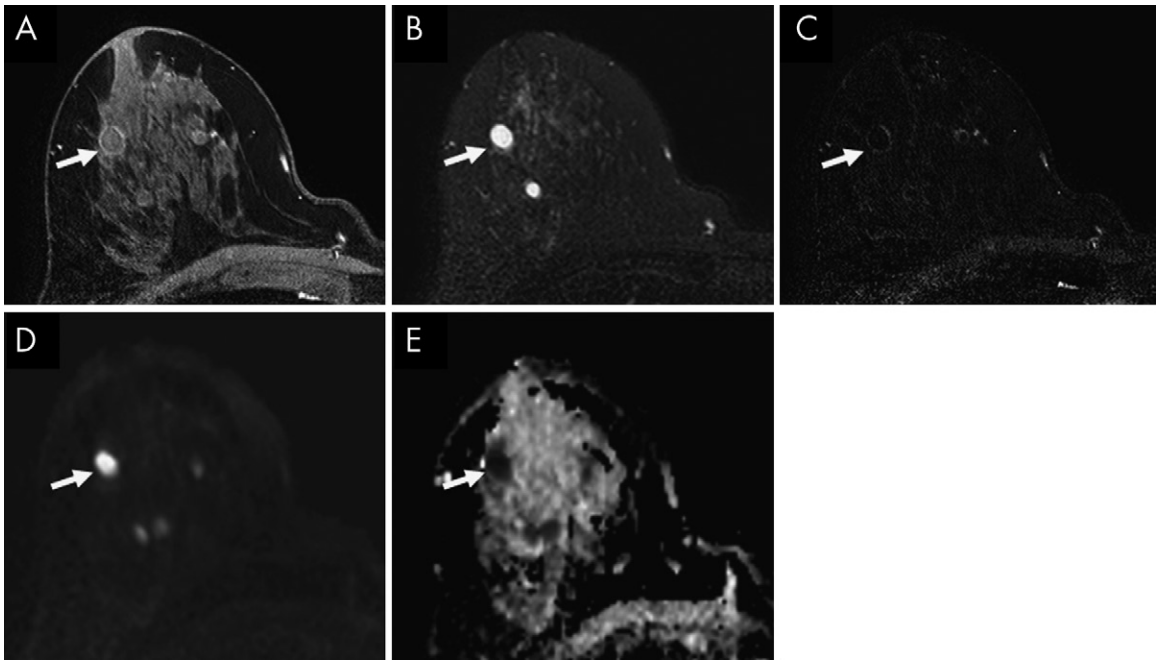

Figure 5: *A–E*, Images in 53-year-old female *BRCA1* mutation carrier with a complicated cyst in the right breast detected at high-risk screening MRI. Axially acquired 3.0-T dynamic contrast-enhanced MRI revealed a 10-mm round mass (arrow) with smooth margins, which is isointense on, *A*, a postcontrast T1-weighted image and hyperintense on, *B*, a T2-weighted image. *C*, Postcontrast T1-weighted subtraction image shows mild rim enhancement and lack of internal enhancement, confirming the diagnosis of complicated cyst (Breast Imaging Reporting and Data System category 2). The mass shows restricted diffusion on, *D*, axially acquired image from diffusion-weighted MRI (b = 800 sec/mm^2) and a low apparent diffusion coefficient (ADC) of 0.48 × 10^{-3} mm^2/sec on, *E*, the corresponding ADC map. If diffusion images were used alone without correlation with dynamic contrast-enhanced MRI and T1-weighted and/or T2-weighted images, this mass would be suspicious. (Reprinted and adapted, with permission, from reference 75.)

titative contrast-to-noise ratio than lower-grade DCIS (51). Therefore, one cannot assume that DW MRI would miss only low-grade DCIS and thus partially remedy the growing concern for overtreatment of DCIS. Nonetheless, DCIS comprised a small proportion of malignancies evaluated by DW MRI reader studies, if not indirectly excluded by exclusion of nonmass enhancement and calcifications (41,53), usual manifestations of DCIS at DCI MRI and mammography, respectively (54–57). Therefore, studies including a greater number of DCIS are needed to adequately evaluate the efficacy of DW MRI in their detection.

In addition, malignant lesions with high water content may also be missed because of their high ADCs. Such lesions include mucinous cancer and triple-negative cancer with extensive necrosis (58,59). For example, among DW MRI blinded reader studies that considered the mucinous subtype of invasive ductal carcinoma separately, mucinous carcinoma was not detected by DW MRI on average 67% of the time (25,41,44,45), with two studies reporting a 100% false-negative rate (25,45).

Last, smaller cancers, specifically ≤ 10–12 mm, were reported to be less detectable in blinded readers studies (23,45). An example of a small invasive ductal carcinoma not detected at DW MRI is shown in Figure E1 (online). This is to be expected given that the typical DW MRI axial in-plane spatial resolution (2 × 2 mm^2) and section thickness (3–5 mm) can result in significant partial volume effect for small lesions, as well as potential obscuration by susceptibility artifact of adjacent biopsy marker clip, which is more pronounced at DW MRI than on conventional T1- or T2-weighted sequences (60). Advanced acquisition techniques described later in this article may in the future improve DW MRI detection of smaller cancers. Additional examples of DW MRI false-negative findings are shown in Figures E2 and E3 (both online).

False-Positive Findings

Less information is available about the nature of DW MRI false-positive findings for a few reasons. First, because these reader studies were performed retrospectively in a setting where DCE MRI is the clinical standard, lesions identified as suspicious at DW MRI alone (DW MRI false-positive findings) were not sampled for biopsy. Therefore, pathology information of DW MRI false-positive findings is known only if they were also found to be suspicious at DCE MRI (DCE MRI false-positive findings) or their appearance could definitively be categorized by DCE MRI (eg, proteinaceous cyst or hematoma).

Among the few DW MRI reader studies that provide pathologic detail of false-positive lesions, the most commonly reported false-positive lesions are complicated/proteinaceous cysts, fibroadenomas, and artifactual "lesions" (23–26,42). In Telegrafo et al, DW MRI falsely depicted seven additional lesions compared with DCE MRI, all of which were found to represent complicated cysts (25). Figure 5 demonstrates a complicated/proteinaceous cyst that may be perceived by a reader as a false-positive finding. Three studies cited fibroadenomas as false-positive findings at DW MRI (24,25,41). An example of fibroadenoma detected at DW MRI is shown in the left breast

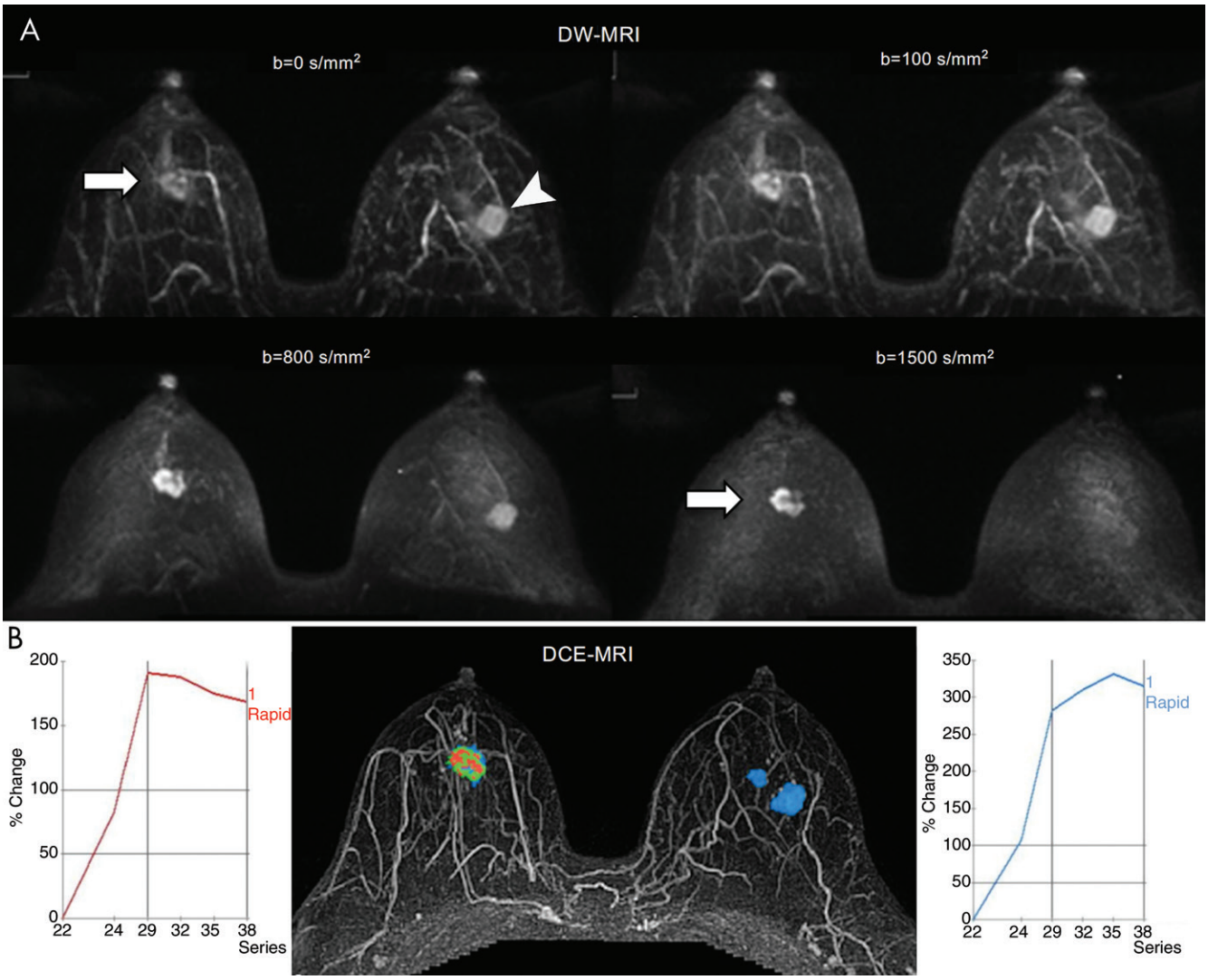

Figure 6: Images in 51-year-old woman with an invasive ductal carcinoma in the right breast (arrow) and a fibroadenoma (arrowhead) in the left breast identified at 3.0-T breast MRI. *A*, Diffusion-weighted (DW) MRI maximum intensity projections generated for axially acquired multiple *b* values (0, 100, 800, and 1500 sec/mm^2 left-to-right and top-to-bottom) show moderate visibility of both masses at $b = 0$ sec/mm^2. However, relative higher signal intensity of the right breast carcinoma occurred with higher *b* values, while relative lower signal intensity of the left breast fibroadenoma occurred with lower *b* values. At $b \leq 800$ sec/mm^2, the left-sided fibroadenoma may be perceived as a suspicious lesion. Apparent diffusion coefficient (ADC) measures (calculated for *b* values of 0 and 1000 sec/mm^2) confirm lower diffusivity in the right carcinoma (ADC = 0.90×10^{-3} mm^2/sec) versus the left fibroadenoma (ADC = 1.54×10^{-3} mm^2/sec). *B*, Axially acquired dynamic contrast-enhanced (DCE) MRI maximum intensity projection with kinetics color map overlay shows an irregular heterogeneously enhancing mass in the right breast with predominantly washout delayed-phase kinetics (red, left curve) corresponding to the carcinoma and an oval mass in the left breast with predominantly persistent delayed-phase kinetics (blue, right curve) corresponding to the fibroadenoma.

lesion in Figure 6. Indeed, fibroadenoma has been found to exhibit a wide range of ADC—up to 37% of fibroadenomas exhibited low ADCs in the same range as malignancies (below an ADC cutoff of 1.81×10^{-3} mm^2/sec) in a prior study of 175 benign breast lesions (61). Fibroadenomas with lower ADCs are found to have higher cellularity and denser stroma than those with higher ADC and more myxoid stroma (62). Last, two reader studies cited examples of artifactual signal at the nipple, an area prone to susceptibility-based distortion at DW MRI (eg, Fig 3), as a cause of false-positive findings (23,24). Regardless, larger prospective studies with tissue sampling for all suspicious lesions found at DW MRI are needed to further understand DW MRI false-positive findings.

Comparison of DW MRI Reader Performance versus Other Modalities

Several of the prior studies explored the comparative and added performance of DW MRI versus other imaging modalities for cancer detection (22–27).

DW MRI versus Mammography

Two studies directly evaluated the benefit of adding DW MRI to mammography as a screening tool. Yabuuchi et al (27) found DW MRI to be more accurate than mammography for detecting breast cancer (area under the receiver operating characteristic curve = 0.73 and 0.64, respectively) and to detect a higher number of cancers compared with mammography alone (sensitivity

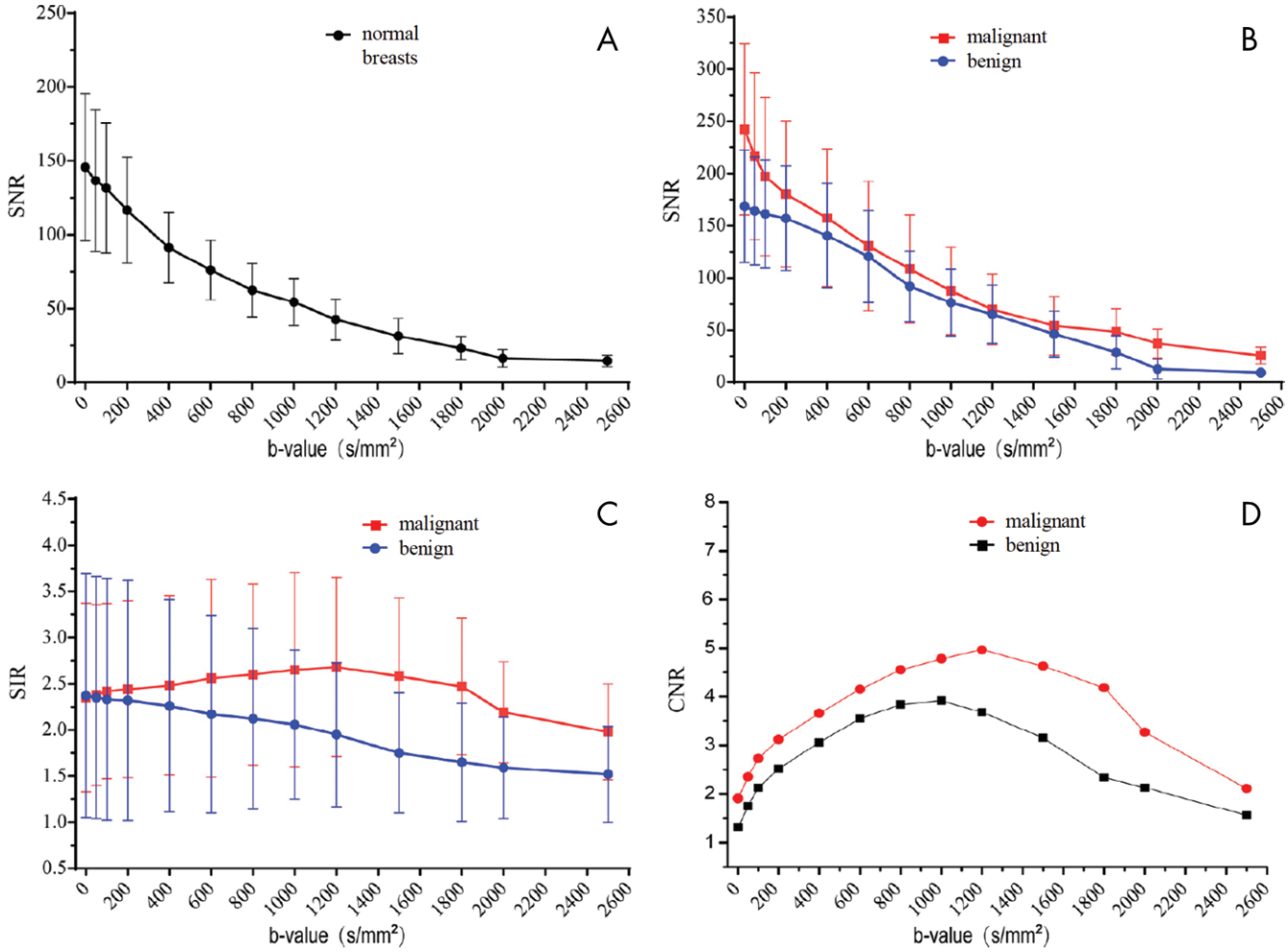

Figure 7: *A–D*, Graphs show diffusion-weighted MRI signal measures of breast tissues across *b* values at 3.0 T. Shown are variations with *b* value in, *A*, mean signal-to-noise ratio (SNR) for normal breasts ($n = 14$), *B*, mean SNR for benign ($n = 72$) and malignant lesions ($n = 40$), *C*, mean signal intensity ratio (SIR) (ie, signal intensity of lesion divided by signal intensity of normal tissue) for benign and malignant lesions, and, *D*, mean contrast-to-noise ratio (CNR) for benign and malignant lesions. All breast lesions in the study were 1.5 cm or larger. The mean CNR values of malignant lesions increased with increasing *b* values up to 1200 sec/mm^2, while SNR continually decreased with increasing *b* values. (Reprinted and adapted, with permission, from reference 63.)

= 69% vs 40%). Similarly, Kazama et al (23) found that combining both modalities improved sensitivity to 93% versus mammography and DW MRI alone (64% and 74% respectively, $P < .01$). Furthermore, although McDonald and colleagues (24) did not evaluate the sensitivity of DW MRI and mammogram in a head-to-head comparison, all malignancies included and detected by DW MRI were mammographically occult. This further highlights the potential improvement in cancer detection by adding DW MRI to routine mammographic screening.

DW MRI versus DCE MRI

In three studies that directly compared the reader performance of DW MRI versus DCE MRI for screening, the average sensitivity of DW MRI was 78.9% (50%–94%) and the average sensitivity of conventional DCE MRI was 93.4% (86%–98%) (22,25,27), with sensitivity significantly different in one (27) but not in the two others (22,25). In the other three studies that used DCE MRI as the reference standard, DW MRI sensitivity was 75.7% (46%–77%) versus DCE MRI sensitivity assumed as 100% (23,24,26). Overall, the results of these studies suggest that the sensitivity of DW MRI for cancer detection in an asymptomatic population is likely lower than that of DCE MRI.

DW MRI versus Abbreviated MRI

Kang et al was the only study of the six that compared DW MRI performance to that of abbreviated MRI. DW MRI performance was reported to be equivalent to the abbreviated MRI, with the added benefit of approximately 10 minutes reduction in image acquisition time and 10 seconds reduction in interpretation time per case (22). Two additional prior studies using DW MRI to detect malignancy in diagnostic clinical scenario reported similar performance between DW MRI and abbreviated MRI (43,46), with one reporting reduction of reading time of negative cases for DW MRI compared with abbreviated MRI (43).

DW MRI versus US

As previously mentioned, nonblinded DW MRI has been suggested to be superior to MRI-guided focused US in can-

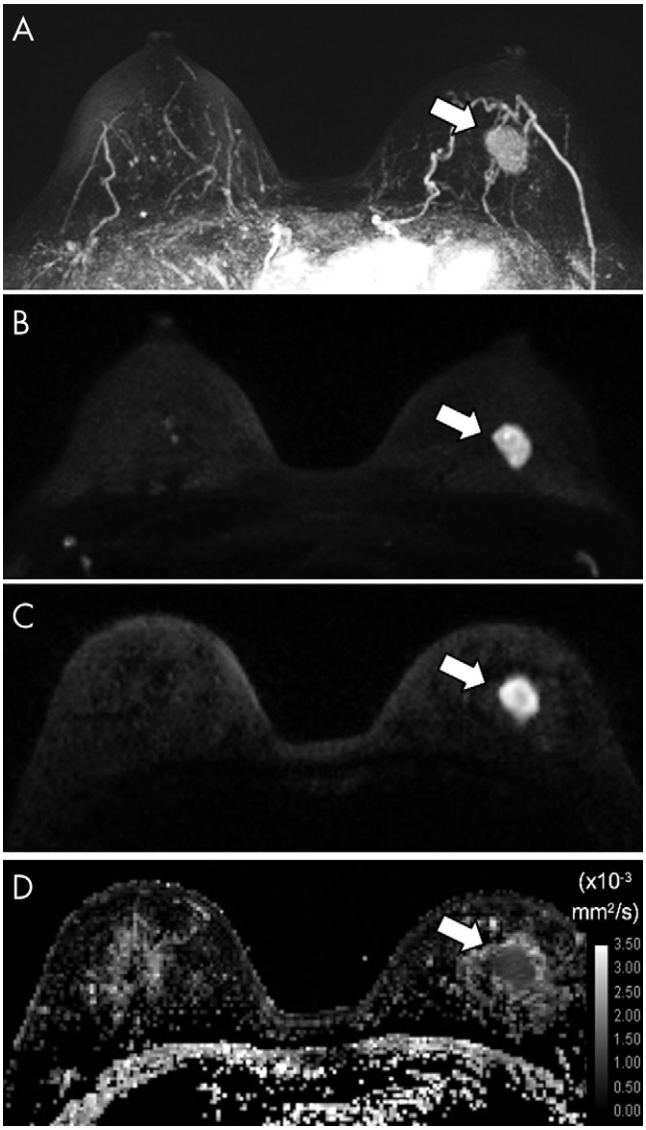

Figure 8: *A–D,* Axial images in 55-year-old woman with left invasive ductal carcinoma of high nuclear and histologic grade identified at 3.0-T breast MRI. *A,* Dynamic contrast-enhanced MRI postcontrast subtraction maximum intensity projection (MIP) shows a mass (arrow), while, *B,* diffusion-weighted (DW) MRI MIP (b = 1000 sec/mm^2), *C,* representative single section from DW MRI (b = 1000 sec/mm^2) through the mass (arrow), and, *D,* apparent diffusion coefficient (ADC) map show corresponding findings. The mass (arrow) exhibited a low mean ADC of 1.04 × 10^{-3} mm^2/sec.

cer detection (37). However, to date, no studies have directly compared blinded DW MRI performance with that of screening whole-breast US, which would be of particular interest due to the growing use of US for supplemental screening in women with dense breasts.

Suggested Image Acquisition and Interpretation Strategies

More studies designed to evaluate DW MRI in screening populations are critical before clinical use of DW MRI as a screening tool can be advocated. What is clear, however, is that determining the true value of DW MRI as a stand-alone screening tool will rely on use of a standardized acquisition protocol and interpretation approach. In this following section, authors present best practice for commonly available DW MRI acquisition technique and interpretation as currently supported by literature, tailored here for the specific application of unenhanced screening.

Protocol

Although a wide range of protocols have been reported in the literature, several acquisition parameters are suggested to ensure adequate breast DW MRI quality. Imaging should be performed in a closed bore magnet at field strength of 1.5 T or higher with maximum gradient strength of at least 30mT/m, using a dedicated breast coil with at least four channels. An EPI-based axial acquisition of bilateral breast should be used, with minimum in-plane resolution of at least 2 × 2 mm^2 and section thickness of 4 mm or less. The echo time should be optimized to be as low as possible and the repetition time should be greater than or equal to 3000 msec. High-quality shimming is essential to minimize field inhomogeneities and resulting susceptibility-based distortions in the EPI images. Parallel imaging must be used to minimize readout echo train lengths (and reduce associated blurring and distortions), with recommended acceleration factor of 2–4. Generation of an ADC map is required.

b Values

Selection of b values is crucial, as b values are known to directly affect image signal-to-noise ratio, lesion contrast-to-noise ratio, and ADCs (63–65). While both the visibility, as reflected quantitatively by contrast-to-noise ratio, and specificity for lesion detection can increase with b value (Figs 6, 7), signal-to-noise ratio decreases (Fig 7), which could limit cancer detection (63,64). Furthermore, acquiring images at higher b values leads to a greater amount of distortion due to susceptibility effects and eddy currents and lengthens imaging times (66). Based on theoretical and observed data, we suggest a maximum b value of 800 sec/mm^2 for accurate estimation of breast ADCs (67,68). Using more than two b values may reduce error in ADC mapping but has not demonstrated any definite diagnostic benefit for differentiation of breast lesions (67,69). However, for screening applications, where both lesion detection and accurate ADC quantitation are priorities, acquiring an additional very high b value of 1200–1500 sec/mm^2 is also recommended to maximize lesion contrast (63,65). Therefore, an acquisition including three b values may be optimal for screening, with a minimum b of 0–50 sec/mm^2, a moderate b of 800 sec/mm^2 for ADC quantitation, and a maximum of approximately 1500 sec/mm^2 for qualitative lesion detection.

The literature identifies several approaches on how to troubleshoot commonly encountered DW MRI challenges and artifacts. Standard DW MRI using single-shot EPI-based sequences is prone to gradient nonlinearity, poor signal-to-noise ratio, and poor fat suppression, which may contribute to DW MRI's lower sensitivity compared with DCE MRI. Gradient nonlinearity, which results in variable ADCs depending on spatial location of the measured region

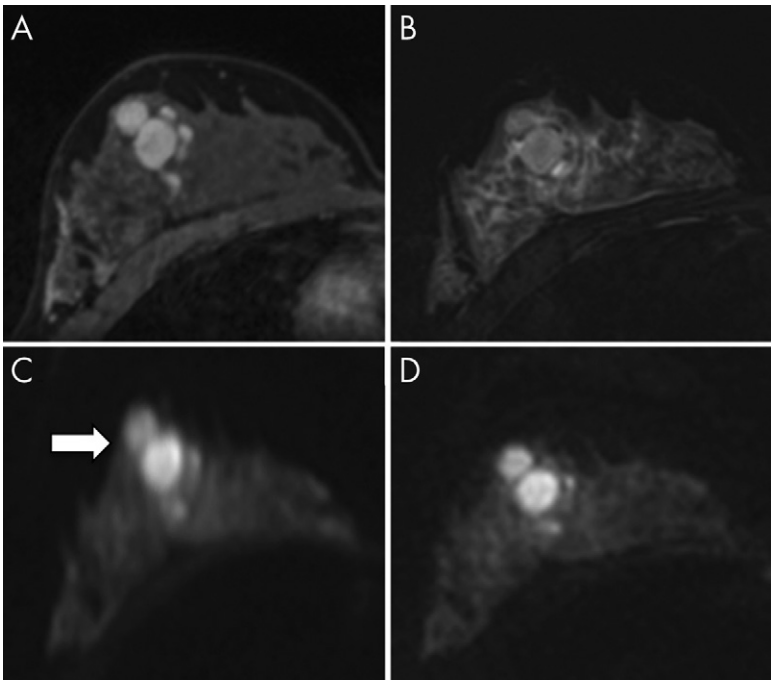

Figure 9: *A–D,* Axial images in 24-year-old woman with fibroadenoma at 3.0-T breast MRI. *A,* Image from T1-weighted dynamic contrast-enhanced MRI, *B,* image from T2-weighted short inversion time inversion recovery MRI, *C,* image from diffusion-weighted (DW) MRI ($b = 850$ sec/mm^2) performed with single-shot echo-planar imaging, and, *D,* readout-segmented echo-planar image. Geometric distortion artifact is seen more prominently on *C* (arrow) than on *D.* (Reprinted, with permission, from reference 79.)

of interest, can be corrected by gradient nonlinearity correction software (70,71). Optimization of signal-to-noise ratio, especially in the setting of the recommended high *b* value, is also recommended by performing preimplementation assessment of image quality and routine calibration with dedicated phantoms with known ADCs. Last, spectral attenuated inversion recovery is recommended to reduce inhomogeneous fat suppression, but, if unsuccessful, short inversion time inversion recovery can also be considered (72).

Interpretation

The general strategy for interpreting breast DW MRI requires both qualitative and quantitative interpretation: first a qualitative (ie, visual) assessment to detect any unique areas of high signal intensity on high-*b*-value DW MRI (indicating impeded diffusion), followed by quantitative assessment of suspicious findings to determine ADCs. This lesion detection and characterization approach is comparable to DCE MRI assessment, where qualitative assessment identifies any suspicious enhancement, and quantitative kinetics metrics provide further information on the likelihood of malignancy. As with either technique, lesion morphology should also be considered and additional information may be obtained from high-resolution unenhanced T2-weighted and T1-weighted anatomic images, if available. Examples of mass and nonmass lesions detected at DW MRI are given in Figures 8 and 4, respectively.

An example that illustrates the need for both a quantitative and a qualitative approach involves "T2-shinethrough." As DW sequences are fundamentally T2 weighted, lesions with high water content may retain high signal on high *b* value regardless of true diffusion impedance. To avoid this pitfall, cross-correlation with the quantitative ADC map is crucial: lesions with true impeded diffusion should exhibit low ADC. In addition, qualitative evaluation of shape (oval) and margin (circumscribed) may be helpful in avoiding misclassification of common false-positive benign lesions such as complicated cysts and fibroadenoma as malignancies (73).

Measuring lesion ADC necessitates drawing a region of interest on the ADC map. The region of interest should ideally be drawn freehand within the solid portion of the lesion, coinciding with the area of suspicious hyperintensity on high-*b*-value DW MRI images, while avoiding normal tissue and areas of necrosis, hemorrhage, or artifact by cross-referencing with unenhanced T1- and T2-weighted images, if available (74,75). While the most common approach is to measure the average ADC across a lesion, some studies suggest that measurement of a small region with the lowest ADC or darkest part within the lesion, representing the most suspicious area, may further improve diagnostic performance (52,74,76,77) and may also be easier to perform with software tools available in clinical settings.

Although different optimal ADC cutoffs have been proposed in literature, a recent multicenter trial has suggested a standardized cutoff above which a lesion is less suspicious, which remains to be further validated. The American College of Radiology Imaging Network 6702 trial explored ADCs of benign and malignant breast lesions across 107 women at 10 academic institutions with varying MR platforms (vendors and field strengths) using a standardized DW MRI protocol. The study confirmed significantly lower mean ADC for malignant versus benign lesions, and that 21% of unnecessary breast biopsies recommended by DCE MRI could be avoided without affecting sensitivity by implementing an ADC cutoff (ADC $> 1.68 \times 10^{-3}$ mm^2/sec for maximum *b* value of 800 sec/mm^2 was suggested).

Advanced Techniques and Postprocessing

Advanced Acquisition Techniques

Future use of DW MRI as a supplemental screening method may be further enhanced by advanced techniques, recently reviewed in depth in the context of breast imaging (29). High-resolution DW MRI could improve sensitivity and allow more accurate characterization of breast lesions, including subcentimeter lesions as previously mentioned. Such techniques include, DW readout-segmented EPI, a multishot EPI approach which reduces the required matrix size acquired per shot (excitation), hence reducing susceptibility artifacts and/or allowing for higher spatial resolution and total image matrix size (22,41,46,78). In breast imaging, readout-segmented EPI was found to reduce geometric distortions

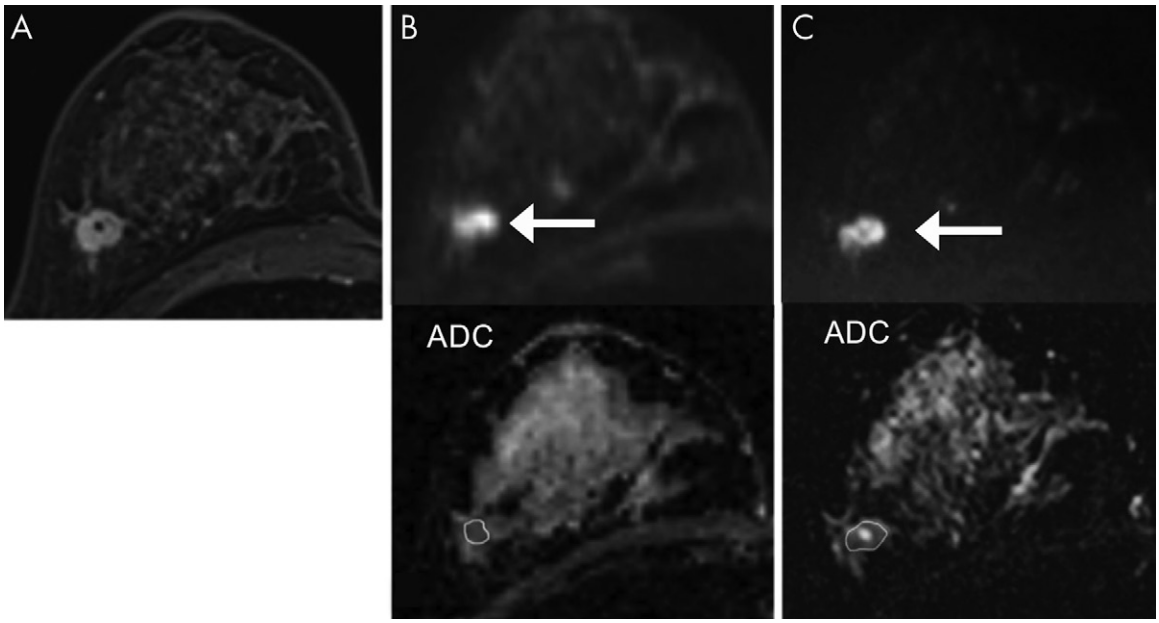

Figure 10: *A–C,* Images in 43-year-old woman with invasive ductal carcinoma in the right breast. *A,* Image from dynamic contrast-enhanced MRI in axial plane shows the biopsy-proven malignant enhancing mass. *B, C (top),* Both readout-segmented echo-planar imaging (EPI) and reduced field of view (rFOV) DW MRI show a mass (arrow) with high signal intensity. In terms of morphologic detail, tumor heterogeneity, and overall image quality, readers preferred rFOV to readout-segmented EPI, while readers found lesion conspicuity comparable for the two techniques. *B, C (bottom),* Apparent diffusion coefficient (ADC) maps from readout-segmented and rFOV MRI show a low-signal-intensity mass (outline), with mean ADCs of 1.29×10^{-3} mm^2/sec for readout-segmented EPI and 0.99×10^{-3} mm^2/sec for rFOV MRI. (Reprinted and adapted, with permission, from reference 83).

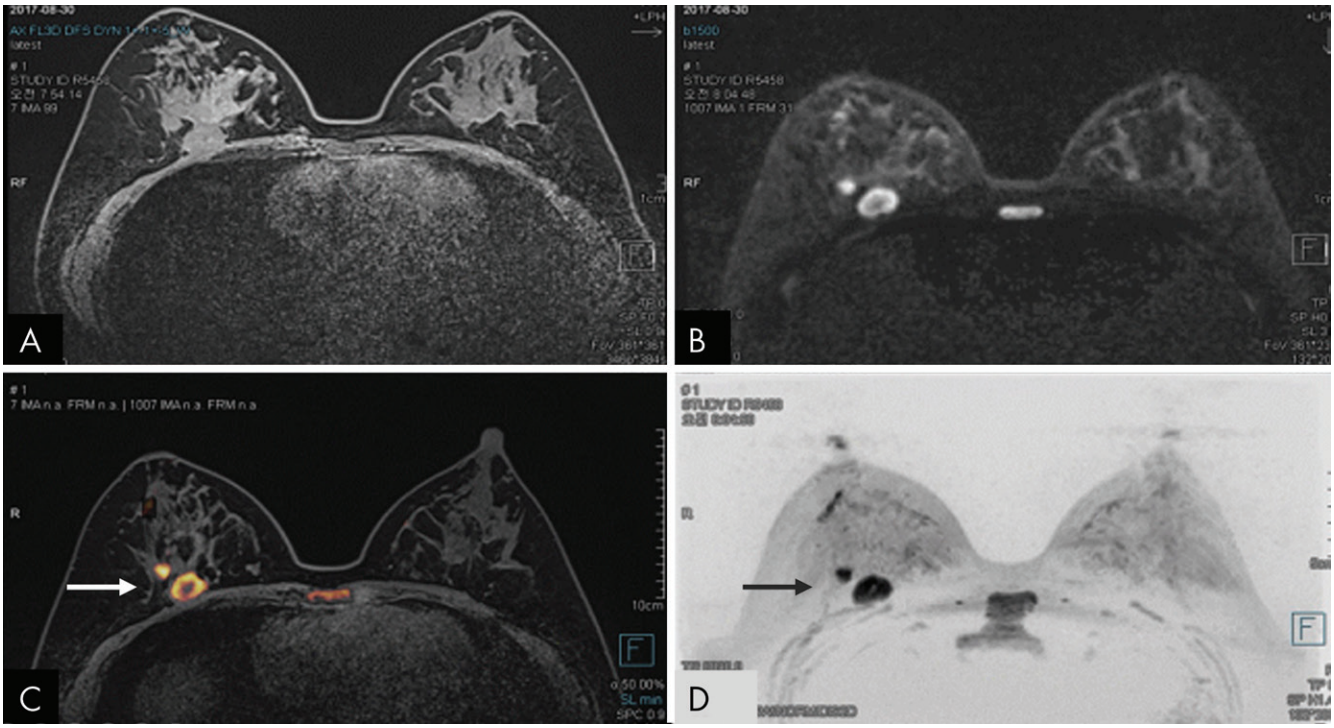

Figure 11: *A–D,* Images in 41-year-old woman with biopsy-proven invasive ductal carcinoma. Fusion of, *A,* axial image from unenhanced T1-weighted MRI performed at 3.0 T and, *B,* axial image from readout-segmented echo-planar imaging diffusion-weighted (DW) MRI (b = 1500 sec/mm^2) obtained by using commercially available Syngo.via software (Siemens Healthcare, Erlangen, Germany) results in, *C,* image from fused DW MRI. In the image from fused DW MRI, the color overlay depicts suspicious regions with high signal intensity at DW MRI (suggesting reduced diffusivity) with detailed anatomic context provided by the underlying T1-weighted MRI, which could help the reader to more accurately assess lesion morphology and location. Both, *C,* image from fused DW MRI and, *D,* DW MRI maximum intensity projection clearly show a suspicious mass with high rim signal intensity and another small nearby suspicious mass in the posterior right breast (arrow).

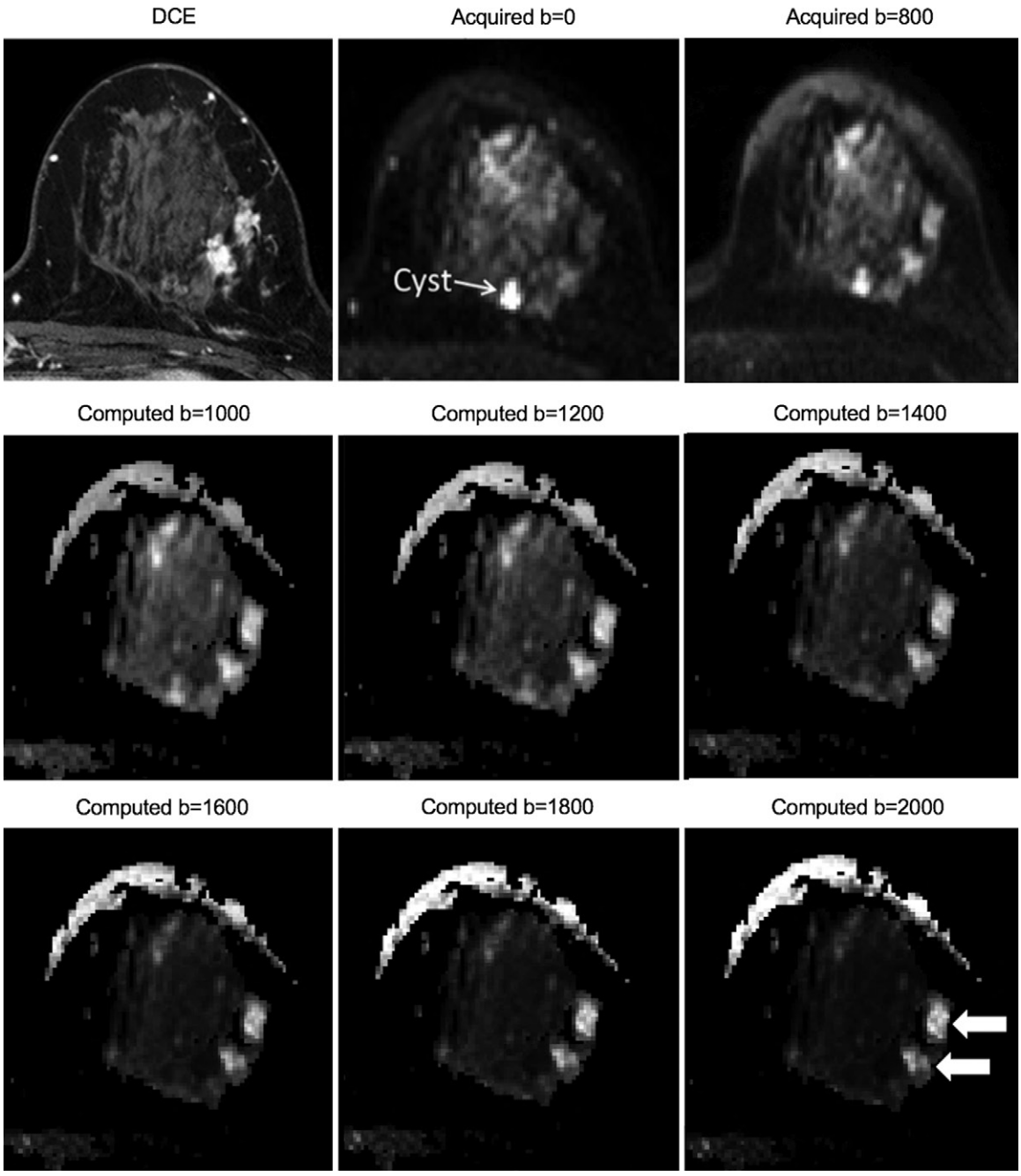

Figure 12: Images in 49-year-old woman with dense breasts and grade 2 invasive ductal carcinoma from 3.0-T breast MRI. Shown left-to-right are (top row) images from (top left image) T1-weighted dynamic contrast-enhanced (DCE) MRI, images from diffusion-weighted (DW) MRI acquired at (top middle image) $b = 0$ sec/mm^2 and (top right image) $b = 800$ sec/mm^2, (middle row) representative computed DW MRI at $b = 1000$, 1200, and 1400 sec/mm^2, and (bottom row) computed DW MRI at $b = 1600$, 1800 sec/mm^2, and 2000 sec/mm^2. Dynamic contrast-enhanced MRI shows two enhancing areas of malignancy. Computed DW MRI at higher b values improves the contrast of the two malignant lesions (arrows) while reducing the relative appearance of a cyst and other high-T2-signal benign tissues, with good overall image quality and signal-to-noise ratio and without longer imaging times.

and T2*-induced blurring versus standard single-shot EPI (79) (Fig 9) and provided higher lesion conspicuity at DW MRI by both qualitative (79) and quantitative assessment (80). Another advanced technique that aims to reduce the required matrix size is reduced field-of-view DW MRI (rFOV), which was judged to improve lesion conspicuity (81) and to provide sharper images for assessing tumor shape and margin (82) compared with full FOV EPI. Furthermore, rFOV may be superior to readout-segmented EPI in lesion conspicuity and image quality (Fig 10) (83). However, absolute ADCs in rFOV DW MRI were lower than when using readout-segmented and standard single-shot EPI techniques ($P < .001$),

which may render prior published ADC cutoffs less useful for interpretation of rFOV DW MRI (82,83).

Postprocessing

Additional solutions utilizing offline postprocessing can help to correct geometric distortions in EPI-based DW MRI arising from field inhomogeneities and other factors. Field mapping approaches and "blip up/down" (phase-encoding polarity reversal) require acquisition of supplementary images to calculate correction maps to "unwarp" susceptibility-related EPI distortions (84–88). Image registration algorithms also can help to reduce spatial inaccuracies and artifacts due to eddy currents, motion, and/or susceptibility effects (89,90).

Other techniques improve cancer conspicuity at DW MRI through enhancing image display. Several studies used maximum intensity projections (MIPs), which can conveniently display DW MRI in a three-dimensional representation as opposed to standard section-by-section evaluation (22,25,43). Similar to conventional postprocessing in breast DCE MRI, DW MRI MIPs are generated by selecting from the multiple sections the axial matrix voxel with the highest signal intensity, resulting in a single image of the whole examination volume. Furthermore, MIPs can reduce reading time and allow for a comparable analysis approach to that used for abbreviated contrast-enhanced MRI protocols (43). Fusion of high-*b*-value DW-MR images to unenhanced T1-weighted or T2-weighted images may also improve accuracy for cancer detection by allowing evaluation of functional diffusion and detailed morphology on the same sequence, similar to PET/CT (Fig 11) (22,46,91). However, potential inaccuracies due to spatial differences of DW MRI versus anatomic images require utilization of advanced approaches to minimize intrinsic EPI geometric distortions.

Last, computed DW MRI is a technique to synthesize high-*b*-value ($b \geq 1500$ sec/mm^2) images from those acquired at a lower *b* values. The technique can provide high-*b*-value images that surpass those acquired directly in terms of image quality and lesion conspicuity (92) (Fig 12) while preserving shorter imaging times and provide flexibility to retrospectively generate images at any *b* value for optimal interpretation.

Advanced Modeling Techniques

Advanced DW MRI modeling techniques hold potential to expand characterization of the tissue microenvironment, which may further increase the clinical value of breast DW MRI. Currently, standard DW MRI (using Gaussian monoexponential modeling) calculates ADCs, which have demonstrated value in differentiating benign from malignant breast lesions (93). However, more sophisticated approaches can reflect additional diffusivity components of the underlying tissue such as perfusion and tissue complexity. An example is intravoxel incoherent motion, which reflects variations in perfusion fractions within tissue that may correspond somewhat to kinetic features detected with DCE MRI (94,95) and can aid in differentiating malignant and benign lesions (96). At high *b* values, diffusion kurtosis modeling can provide further insight into tissue complexity and improve breast lesion characterization over standard ADC values (97). Diffusion-tensor imaging is another advanced technique, which probes water motion in six or more directions to characterize diffusion directionality and may reflect alterations in glandular microstructural organization. Preliminary studies suggest diffusion-tensor imaging could incrementally improve sensitivity for identifying cancer in the breast over standard DW MRI (98,99). The aforementioned advanced techniques, while not routinely used in clinical breast imaging, are areas of active exploration with promise to provide valuable new imaging biomarkers in the near future.

Conclusion

In summary, diffusion-weighted (DW) MRI is a fast, unenhanced modality that shows promise in identifying mammographically occult malignancy and warrants further investigation as an alternative supplemental breast cancer screening tool. Results of multiple studies suggest that DW MRI may have sensitivity lower than that of DCE MRI but perhaps superior to that of mammography and US. Moreover, the ability of DW MRI to detect cancer may further be enhanced using the optimal acquisition and interpretation protocols suggested in this review. Additional DW MRI investigations using standardized approaches in larger patient cohorts are essential prior to widespread implementation. However, given the potential improvement in convenience and safety, an unenhanced MRI screening technique like DW MRI represents a promising alternative for improving breast cancer detection.

Disclosures of Conflicts of Interest: N.A. disclosed no relevant relationships. **S.B.** Activities related to the present article: disclosed no relevant relationships. Activities not related to the present article: is on the speakers bureau of Siemens Healthineers. Other relationships: with institution, has two patents pending in the field of diffusion-weighted imaging. **H.J.S.** disclosed no relevant relationships. **M.D.** disclosed no relevant relationships. **H.R.** Activities related to the present article: institution has received a grant from GE Healthcare. Activities not related to the present article: disclosed no relevant relationships. Other relationships: disclosed no relevant relationships. **K.P.** Activities related to the present article: disclosed no relevant relationships. Activities not related to the present article: institution has received grants from the EU Framework Programme for Research and Innovation; has given lectures on MRI for the European Society of Breast Imaging. Other relationships: disclosed no relevant relationships. **S.C.P.** Activities related to the present article: is a consultant for Seoul National University Hospital on a national diffusion-weighted imaging screening trial protocol development program; institution has received in-kind research and technical support from Philips Healthcare for the development and testing of advanced breast diffusion-weighted imaging sequences; institution has received pilot grants from the Safeway Foundation, the Wings of Karen Foundation, and *Earlier.org*. Activities not related to the present article: institution has received grants from GE Healthcare. Other relationships: disclosed no relevant relationships.

References

1. Oeffinger KC, Fontham ET, Etzioni R, et al. Breast Cancer Screening for Women at Average Risk: 2015 Guideline Update From the American Cancer Society. JAMA 2015;314(15):1599–1614.
2. Carney PA, Miglioretti DL, Yankaskas BC, et al. Individual and combined effects of age, breast density, and hormone replacement therapy use on the accuracy of screening mammography. Ann Intern Med 2003;138(3):168–175.
3. Saslow D, Boetes C, Burke W, et al. American Cancer Society guidelines for breast screening with MRI as an adjunct to mammography. CA Cancer J Clin 2007;57(2):75–89.

4. Lehman CD, Blume JD, Weatherall P, et al. Screening women at high risk for breast cancer with mammography and magnetic resonance imaging. Cancer 2005;103(9):1898–1905.
5. Mann RM, Kuhl CK, Kinkel K, Boetes C. Breast MRI: guidelines from the European Society of Breast Imaging. Eur Radiol 2008;18(7):1307–1318.
6. U.S. Centers for Medicare & Medicaid Services. Physician Fee Schedule Search. https://www.cms.gov/apps/physician-fee-schedule/search/search-results.aspx?Y=0&T=0&HT=0&CT=1&H1=77049&C=1&M=5. Published January 11, 2019. Accessed March 30, 2019.
7. American College of Radiology. Breast Magnetic Resonance Imaging (MRI) Accreditation Program Requirements. https://www.acraccreditation.org/-/media/ACRAccreditation/Documents/Breast-MRI/Requirements.pdf?la=en. Published October 4, 2017. Accessed June 6, 2019.
8. Kuhl CK, Schrading S, Strobel K, Schild HH, Hilgers RD, Bieling HB. Abbreviated breast magnetic resonance imaging (MRI): first postcontrast subtracted images and maximum-intensity projection-a novel approach to breast cancer screening with MRI. J Clin Oncol 2014;32(22):2304–2310.
9. Leithner D, Moy L, Morris EA, Marino MA, Helbich TH, Pinker K. Abbreviated MRI of the Breast: Does It Provide Value? J Magn Reson Imaging 2019;49(7):e85–e100.
10. Petrillo A, Fusco R, Sansone M, et al. Abbreviated breast dynamic contrast-enhanced MR imaging for lesion detection and characterization: the experience of an Italian oncologic center. Breast Cancer Res Treat 2017;164(2):401–410.
11. Behzadi AH, Zhao Y, Farooq Z, Prince MR. Immediate Allergic Reactions to Gadolinium-based Contrast Agents: A Systematic Review and Meta-Analysis. Radiology 2018;286(2):731.
12. Nicholas BA, Vricella GJ, Smith M, Passalacqua M, Gulani V, Ponsky LE. Contrast-induced nephropathy and nephrogenic systemic fibrosis: minimizing the risk. Can J Urol 2012;19(1):6074–6080.
13. Garcia-Bournissen F, Shrim A, Koren G. Safety of gadolinium during pregnancy. Can Fam Physician 2006;52:309–310.
14. Kanda T, Fukusato T, Matsuda M, et al. Gadolinium-based Contrast Agent Accumulates in the Brain Even in Subjects without Severe Renal Dysfunction: Evaluation of Autopsy Brain Specimens with Inductively Coupled Plasma Mass Spectroscopy. Radiology 2015;276(1):228–232.
15. Gulani V, Calamante F, Shellock FG, Kanal E, Reeder SB; International Society for Magnetic Resonance in Medicine. Gadolinium deposition in the brain: summary of evidence and recommendations. Lancet Neurol 2017;16(7):564–570.
16. McDonald RJ, McDonald JS, Kallmes DF, et al. Intracranial Gadolinium Deposition after Contrast-enhanced MR Imaging. Radiology 2015;275(3):772–782.
17. Hooley RJ, Greenberg KL, Stackhouse RM, Geisel JL, Butler RS, Philpotts LE. Screening US in patients with mammographically dense breasts: initial experience with Connecticut Public Act 09-41. Radiology 2012;265(1):59–69.
18. Parris T, Wakefield D, Frimmer H. Real world performance of screening breast ultrasound following enactment of Connecticut Bill 458. Breast J 2013;19(1):64–70.
19. Berg WA, Blume JD, Cormack JB, et al. Combined screening with ultrasound and mammography vs mammography alone in women at elevated risk of breast cancer. JAMA 2008;299(18):2151–2163.
20. Sprague BL, Stout NK, Schechter C, et al. Benefits, harms, and cost-effectiveness of supplemental ultrasonography screening for women with dense breasts. Ann Intern Med 2015;162(3):157–166.
21. Ohuchi N, Suzuki A, Sobue T, et al. Sensitivity and specificity of mammography and adjunctive ultrasonography to screen for breast cancer in the Japan Strategic Anti-cancer Randomized Trial (J-START): a randomised controlled trial. Lancet 2016;387(10016):341–348.
22. Kang JW, Shin HJ, Shin KC, et al. Unenhanced magnetic resonance screening using fused diffusion-weighted imaging and maximum-intensity projection in patients with a personal history of breast cancer: role of fused DWI for postoperative screening. Breast Cancer Res Treat 2017;165(1):119–128.
23. Kazama T, Kuroki Y, Kikuchi M, et al. Diffusion-weighted MRI as an adjunct to mammography in women under 50 years of age: an initial study. J Magn Reson Imaging 2012;36(1):139–144.
24. McDonald ES, Hammersley JA, Chou SH, et al. Performance of DWI as a Rapid Unenhanced Technique for Detecting Mammographically Occult Breast Cancer in Elevated-Risk Women With Dense Breasts. AJR Am J Roentgenol 2016;207(1):205–216.
25. Telegrafo M, Rella L, Stabile Ianora AA, Angelelli G, Moschetta M. Unenhanced breast MRI (STIR, T2-weighted TSE, DWIBS): An accurate and alternative strategy for detecting and differentiating breast lesions. Magn Reson Imaging 2015;33(8):951–955.
26. Trimboli RM, Verardi N, Cartia F, Carbonaro LA, Sardanelli F. Breast cancer detection using double reading of unenhanced MRI including T1-weighted, T2-weighted STIR, and diffusion-weighted imaging: a proof of concept study. AJR Am J Roentgenol 2014;203(3):674–681.
27. Yabuuchi H, Matsuo Y, Sunami S, et al. Detection of non-palpable breast cancer in asymptomatic women by using unenhanced diffusion-weighted and T2-weighted MR imaging: comparison with mammography and dynamic contrast-enhanced MR imaging. Eur Radiol 2011;21(1):11–17.
28. Le Bihan D, Breton E, Lallemand D, Grenier P, Cabanis E, Laval-Jeantet M. MR imaging of intravoxel incoherent motions: application to diffusion and perfusion in neurologic disorders. Radiology 1986;161(2):401–407.
29. Partridge SC, Nissan N, Rahbar H, Kitsch AE, Sigmund EE. Diffusion-weighted breast MRI: Clinical applications and emerging techniques. J Magn Reson Imaging 2017;45(2):337–355.
30. Yoshikawa MI, Ohsumi S, Sugata S, et al. Relation between cancer cellularity and apparent diffusion coefficient values using diffusion-weighted magnetic resonance imaging in breast cancer. Radiat Med 2008;26(4):222–226.
31. Jiang R, Ma Z, Dong H, Sun S, Zeng X, Li X. Diffusion tensor imaging of breast lesions: evaluation of apparent diffusion coefficient and fractional anisotropy and tissue cellularity. Br J Radiol 2016;89(1064):20160076.
32. Chen L, Liu M, Bao J, et al. The correlation between apparent diffusion coefficient and tumor cellularity in patients: a meta-analysis. PLoS One 2013;8(11):e79008.
33. Peters NH, Borel Rinkes IH, Zuithoff NP, Mali WP, Moons KG, Peeters PH. Meta-analysis of MR imaging in the diagnosis of breast lesions. Radiology 2008;246(1):116–124.
34. Lehman CD, Arao RF, Sprague BL, et al. National Performance Benchmarks for Modern Screening Digital Mammography: Update from the Breast Cancer Surveillance Consortium. Radiology 2017;283(1):49–58.
35. Zhang L, Tang M, Min Z, Lu J, Lei X, Zhang X. Accuracy of combined dynamic contrast-enhanced magnetic resonance imaging and diffusion-weighted imaging for breast cancer detection: a meta-analysis. Acta Radiol 2016;57(6):651–660.
36. Partridge SC, Demartini WB, Kurland BF, Eby PR, White SW, Lehman CD. Differential diagnosis of mammographically and clinically occult breast lesions on diffusion-weighted MRI. J Magn Reson Imaging 2010;31(3):562–570.
37. Amornsiripanitch N, Rahbar H, Kitsch AE, Lam DL, Weitzel B, Partridge SC. Visibility of mammographically occult breast cancer on diffusion-weighted MRI versus ultrasound. Clin Imaging 2018;49:37–43.
38. Hahn SY, Ko ES, Han BK, Lim Y, Gu S, Ko EY. Analysis of factors influencing the degree of detectability on diffusion-weighted MRI and diffusion background signals in patients with invasive breast cancer. Medicine (Baltimore) 2016;95(27):e4086.
39. Horvat JV, Durando M, Milans S, et al. Apparent diffusion coefficient mapping using diffusion-weighted MRI: impact of background parenchymal enhancement, amount of fibroglandular tissue and menopausal status on breast cancer diagnosis. Eur Radiol 2018;28(6):2516–2524.
40. Baltzer PA, Benndorf M, Dietzel M, Gajda M, Camara O, Kaiser WA. Sensitivity and specificity of unenhanced MR mammography (DWI combined with T2-weighted TSE imaging, ueMRM) for the differentiation of mass lesions. Eur Radiol 2010;20(5):1101–1110.
41. Baltzer PAT, Bickel H, Spick C, et al. Potential of Noncontrast Magnetic Resonance Imaging With Diffusion-Weighted Imaging in Characterization of Breast Lesions: Intraindividual Comparison With Dynamic Contrast-Enhanced Magnetic Resonance Imaging. Invest Radiol 2018;53(4):229–235.
42. Belli P, Bufi E, Bonatesta A, et al. Unenhanced breast magnetic resonance imaging: detection of breast cancer. Eur Rev Med Pharmacol Sci 2016;20(20):4220–4229.
43. Bickelhaupt S, Laun FB, Tesdorff J, et al. Fast and Noninvasive Characterization of Suspicious Lesions Detected at Breast Cancer X-Ray Screening: Capability of Diffusion-weighted MR Imaging with MIPs. Radiology 2016;278(3):689–697.
44. Kuroki-Suzuki S, Kuroki Y, Nasu K, Nawano S, Moriyama N, Okazaki M. Detecting breast cancer with non-contrast MR imaging: combining diffusion-weighted and STIR imaging. Magn Reson Med Sci 2007;6(1):21–27.
45. Pinker K, Moy L, Sutton EJ, et al. Diffusion-Weighted Imaging With Apparent Diffusion Coefficient Mapping for Breast Cancer Detection as a Stand-Alone Parameter: Comparison With Dynamic Contrast-Enhanced and Multiparametric Magnetic Resonance Imaging. Invest Radiol 2018;53(10):587–595.
46. Shin HJ, Chae EY, Choi WJ, et al. Diagnostic Performance of Fused Diffusion-Weighted Imaging Using Unenhanced or Postcontrast T1-Weighted MR Imaging in Patients With Breast Cancer. Medicine (Baltimore) 2016;95(17):e3502.
47. Wu LM, Chen J, Hu J, Gu HY, Xu JR, Hua J. Diffusion-weighted magnetic resonance imaging combined with T2-weighted images in the detection of small breast cancer: a single-center multi-observer study. Acta Radiol 2014;55(1):24–31.

48. Yoshikawa MI, Ohsumi S, Sugata S, et al. Comparison of breast cancer detection by diffusion-weighted magnetic resonance imaging and mammography. Radiat Med 2007;25(5):218–223.
49. Anderson SJ, Wapnir I, Dignam JJ, et al. Prognosis after ipsilateral breast tumor recurrence and locoregional recurrences in patients treated by breast-conserving therapy in five National Surgical Adjuvant Breast and Bowel Project protocols of node-negative breast cancer. J Clin Oncol 2009;27(15):2466–2473.
50. Choi SY, Chang YW, Park HJ, Kim HJ, Hong SS, Seo DY. Correlation of the apparent diffusion coefficiency values on diffusion-weighted imaging with prognostic factors for breast cancer. Br J Radiol 2012;85(1016):e474–e479.
51. Rahbar H, Partridge SC, Eby PR, et al. Characterization of ductal carcinoma in situ on diffusion weighted breast MRI. Eur Radiol 2011;21(9):2011–2019.
52. Iima M, Le Bihan D, Okumura R, et al. Apparent diffusion coefficient as an MR imaging biomarker of low-risk ductal carcinoma in situ: a pilot study. Radiology 2011;260(2):364–372.
53. Baltzer PA, Schäfer A, Dietzel M, et al. Diffusion tensor magnetic resonance imaging of the breast: a pilot study. Eur Radiol 2011;21(1):1–10.
54. Barreau B, de Mascarel I, Feuga C, et al. Mammography of ductal carcinoma in situ of the breast: review of 909 cases with radiographic-pathologic correlations. Eur J Radiol 2005;54(1):55–61.
55. Jansen SA, Newstead GM, Abe H, Shimauchi A, Schmidt RA, Karczmar GS. Pure ductal carcinoma in situ: kinetic and morphologic MR characteristics compared with mammographic appearance and nuclear grade. Radiology 2007;245(3):684–691.
56. Menell JH, Morris EA, Dershaw DD, Abramson AF, Brogi E, Liberman L. Determination of the presence and extent of pure ductal carcinoma in situ by mammography and magnetic resonance imaging. Breast J 2005;11(6):382–390.
57. Rosen EL, Smith-Foley SA, DeMartini WB, Eby PR, Peacock S, Lehman CD. BI-RADS MRI enhancement characteristics of ductal carcinoma in situ. Breast J 2007;13(6):545–550.
58. Woodhams R, Matsunaga K, Kan S, et al. ADC mapping of benign and malignant breast tumors. Magn Reson Med Sci 2005;4(1):35–42.
59. Youk JH, Son EJ, Chung J, Kim JA, Kim EK. Triple-negative invasive breast cancer on dynamic contrast-enhanced and diffusion-weighted MR imaging: comparison with other breast cancer subtypes. Eur Radiol 2012;22(8):1724–1734.
60. Le Bihan D, Poupon C, Amadon A, Lethimonnier F. Artifacts and pitfalls in diffusion MRI. J Magn Reson Imaging 2006;24(3):478–488.
61. Parsian S, Rahbar H, Allison KH, et al. Nonmalignant breast lesions: ADCs of benign and high-risk subtypes assessed as false-positive at dynamic enhanced MR imaging. Radiology 2012;265(3):696–706.
62. Parsian S, Giannakopoulos NV, Rahbar H, Rendi MH, Chai X, Partridge SC. Diffusion-weighted imaging reflects variable cellularity and stromal density present in breast fibroadenomas. Clin Imaging 2016;40(5):1047–1054.
63. Han X, Li J, Wang X. Comparison and Optimization of 3.0 T Breast Images Quality of Diffusion-Weighted Imaging with Multiple B-Values. Acad Radiol 2017;24(4):418–425.
64. Iima M, Yano K, Kataoka M, et al. Quantitative non-Gaussian diffusion and intravoxel incoherent motion magnetic resonance imaging: differentiation of malignant and benign breast lesions. Invest Radiol 2015;50(4):205–211.
65. Tamura T, Murakami S, Naito K, Yamada T, Fujimoto T, Kikkawa T. Investigation of the optimal b-value to detect breast tumors with diffusion weighted imaging by 1.5-T MRI. Cancer Imaging 2014;14:11.
66. Nilsson M, Szczepankiewicz F, van Westen D, Hansson O. Extrapolation-Based References Improve Motion and Eddy-Current Correction of High B-Value DWI Data: Application in Parkinson's Disease Dementia. PLoS One 2015;10(11):e0141825.
67. Bogner W, Gruber S, Pinker K, et al. Diffusion-weighted MR for differentiation of breast lesions at 3.0 T: how does selection of diffusion protocols affect diagnosis? Radiology 2009;253(2):341–351.
68. Dorrius MD, Dijkstra H, Oudkerk M, Sijens PE. Effect of b value and pre-admission of contrast on diagnostic accuracy of 1.5-T breast DWI: a systematic review and meta-analysis. Eur Radiol 2014;24(11):2835–2847.
69. Peters NH, Vincken KL, van den Bosch MA, Luijten PR, Mali WP, Bartels LW. Quantitative diffusion weighted imaging for differentiation of benign and malignant breast lesions: the influence of the choice of b-values. J Magn Reson Imaging 2010;31(5):1100–1105.
70. Tan ET, Marinelli L, Slavens ZW, King KF, Hardy CJ. Improved correction for gradient nonlinearity effects in diffusion-weighted imaging. J Magn Reson Imaging 2013;38(2):448–453.
71. Newitt DC, Tan ET, Wilmes LJ, et al. Gradient nonlinearity correction to improve apparent diffusion coefficient accuracy and standardization in the american college of radiology imaging network 6698 breast cancer trial. J Magn Reson Imaging 2015;42(4):908–919.
72. Nogueira L, Brandão S, Matos E, et al. Diffusion-weighted breast imaging at 3 T: preliminary experience. Clin Radiol 2014;69(4):378–384.
73. Radovic N, Ivanac G, Divjak E, Biondic I, Bulum A, Brkljacic B. Evaluation of Breast Cancer Morphology Using Diffusion-Weighted and Dynamic Contrast-Enhanced MRI: Intermethod and Interobserver Agreement. J Magn Reson Imaging 2019;49(5):1381–1390.
74. Bickel H, Pinker K, Polanec S, et al. Diffusion-weighted imaging of breast lesions: Region-of-interest placement and different ADC parameters influence apparent diffusion coefficient values. Eur Radiol 2017;27(5):1883–1892.
75. Partridge SC, McDonald ES. Diffusion weighted magnetic resonance imaging of the breast: protocol optimization, interpretation, and clinical applications. Magn Reson Imaging Clin N Am 2013;21(3):601–624.
76. Nogueira L, Brandão S, Matos E, et al. Region of interest demarcation for quantification of the apparent diffusion coefficient in breast lesions and its interobserver variability. Diagn Interv Radiol 2015;21(2):123–127.
77. Arponen O, Sudah M, Masarwah A, et al. Diffusion-Weighted Imaging in 3.0 Tesla Breast MRI: Diagnostic Performance and Tumor Characterization Using Small Subregions vs. Whole Tumor Regions of Interest. PLoS One 2015;10(10):e0138702.
78. Porter DA, Heidemann RM. High resolution diffusion-weighted imaging using readout-segmented echo-planar imaging, parallel imaging and a two-dimensional navigator-based reacquisition. Magn Reson Med 2009;62(2):468–475.
79. Bogner W, Pinker-Domenig K, Bickel H, et al. Readout-segmented echo-planar imaging improves the diagnostic performance of diffusion-weighted MR breast examinations at 3.0 T. Radiology 2012;263(1):64–76.
80. Wisner DJ, Rogers N, Deshpande VS, et al. High-resolution diffusion-weighted imaging for the separation of benign from malignant BI-RADS 4/5 lesions found on breast MRI at 3T. J Magn Reson Imaging 2014;40(3):674–681.
81. Singer L, Wilmes LJ, Saritas EU, et al. High-resolution diffusion-weighted magnetic resonance imaging in patients with locally advanced breast cancer. Acad Radiol 2012;19(5):526–534.
82. Barentsz MW, Taviani V, Chang JM, et al. Assessment of tumor morphology on diffusion-weighted (DWI) breast MRI: Diagnostic value of reduced field of view DWI. J Magn Reson Imaging 2015;42(6):1656–1665.
83. Park JY, Shin HJ, Shin KC, et al. Comparison of readout segmented echo planar imaging (EPI) and EPI with reduced field-of-VIew diffusion-weighted imaging at 3t in patients with breast cancer. J Magn Reson Imaging 2015;42(6):1679–1688.
84. Jezzard P, Balaban RS. Correction for geometric distortion in echo planar images from B0 field variations. Magn Reson Med 1995;34(1):65–73.
85. Teruel JR, Fjøsne HE, Østlie A, et al. Inhomogeneous static magnetic field-induced distortion correction applied to diffusion weighted MRI of the breast at 3T. Magn Reson Med 2015;74(4):1138–1144.
86. Andersson JL, Skare S, Ashburner J. How to correct susceptibility distortions in spin-echo echo-planar images: application to diffusion tensor imaging. Neuroimage 2003;20(2):870–888.
87. Hancu I, Lee SK, Hulsey K, et al. Distortion correction in diffusion-weighted imaging of the breast: Performance assessment of prospective, retrospective, and combined (prospective + retrospective) approaches. Magn Reson Med 2017;78(1):247–253.
88. van Rijssel MJ, Zijlstra F, Seevinck PR, et al. Reducing distortions in echo-planar breast imaging at ultrahigh field with high-resolution off-resonance maps. Magn Reson Med 2019;82(1):425–435.
89. Arlinghaus LR, Welch EB, Chakravarthy AB, et al. Motion correction in diffusion-weighted MRI of the breast at 3T. J Magn Reson Imaging 2011;33(5):1063–1070.
90. Takatsu Y, Sagawa H, Nakamura M, Suzuki Y, Miyati T. Novel distortion correction method for diffusion-weighted imaging based on non-rigid image registration between low b value image and anatomical image. Magn Reson Imaging 2019;57:277–284.
91. Bickelhaupt S, Tesdorff J, Laun FB, et al. Independent value of image fusion in unenhanced breast MRI using diffusion-weighted and morphological T2-weighted images for lesion characterization in patients with recently detected BI-RADS 4/5 x-ray mammography findings. Eur Radiol 2017;27(2):562–569.
92. O'Flynn EA, Blackledge M, Collins D, et al. Evaluating the diagnostic sensitivity of computed diffusion-weighted MR imaging in the detection of breast cancer. J Magn Reson Imaging 2016;44(1):130–137.
93. Chen X, Li WL, Zhang YL, Wu Q, Guo YM, Bai ZL. Meta-analysis of quantitative diffusion-weighted MR imaging in the differential diagnosis of breast lesions. BMC Cancer 2010;10(1):693.
94. Iima M, Kataoka M, Kanao S, et al. Intravoxel Incoherent Motion and Quantitative Non-Gaussian Diffusion MR Imaging: Evaluation of the Di-

agnostic and Prognostic Value of Several Markers of Malignant and Benign Breast Lesions. Radiology 2018;287(2):432–441.
95. Song SE, Cho KR, Seo BK, et al. Intravoxel incoherent motion diffusion-weighted MRI of invasive breast cancer: Correlation with prognostic factors and kinetic features acquired with computer-aided diagnosis. J Magn Reson Imaging 2019;49(1):118–130.
96. Cho GY, Moy L, Kim SG, et al. Evaluation of breast cancer using intravoxel incoherent motion (IVIM) histogram analysis: comparison with malignant status, histological subtype, and molecular prognostic factors. Eur Radiol 2016;26(8):2547–2558.
97. Bickelhaupt S, Jaeger PF, Laun FB, et al. Radiomics Based on Adapted Diffusion Kurtosis Imaging Helps to Clarify Most Mammographic Findings Suspicious for Cancer. Radiology 2018;287(3):761–770.
98. Partridge SC, Ziadloo A, Murthy R, et al. Diffusion tensor MRI: preliminary anisotropy measures and mapping of breast tumors. J Magn Reson Imaging 2010;31(2):339–347.
99. Furman-Haran E, Grobgeld D, Nissan N, Shapiro-Feinberg M, Degani H. Can diffusion tensor anisotropy indices assist in breast cancer detection? J Magn Reson Imaging 2016;44(6):1624–1632.